SEMARAK ILMU PUBLISHING

Journal of Advanced Research in Applied Mechanics

Journal homepage:
https://semarakilmu.com.my/journals/index.php/appl_mech/index
ISSN: 2289-7895

The Influence of TiC Dispersion and Density on the Microstructural Features and Microhardness Fused by TIG Arc Process

Md Abd Maleque[1,*], Ahmed Nazrin Md Idriss[1], Rosmia Naping[1], Md Mustafizur Rahman[2], Ihsan Efeoglu[3]

[1] Department of Manufacturing and Materials Engineering, Kulliyah of Engineering, International Islamic University of Malaysia, PO Box 10, 50728, Kuala Lumpur, Malaysia
[2] College of Engineering, Universiti Malaysia Pahang, 26300 Pahang, Malaysia
[3] Faculty of Engineering, Department of Mechanical Engineering, Atatürk University, 25240 Erzurum, Türkiye

ARTICLE INFO

Article history:
Received 13 October 2023
Received in revised form 15 December 2023
Accepted 2 January 2024
Available online 23 February 2024

Keywords:
TIG arc; TiC; Steel; Preplace

ABSTRACT

Surface hardening is a technique to modify a thin layer on the substrate serving the purpose to resist annihilation from the wear and corrosion conditions. In this work titanium carbide (TiC) particulates was incorporated on the surface of the AISI 4340 low alloy steel at different content and heat inputs using the tungsten inert gas (TIG) melting process. The examined melt sizes, microstructures, defects and microhardness were reported. It was found that all tracks were free from crack defects with each track possessing sound metallurgical bonding to the substrate. The containment of majority undissolved TiC followed by the reprecipitated ones were densed when melting was conducted at 2160 J/mm between 1mg/mm^2 to 2 mg/mm^2 powder. The reprecipitated mostly the globular and flower type microstructures were seen dispersed and surrounded by overwhelmingly more of the Fe matrix fused at 1008 J/mm between 0.4 mg/mm^2 to 0.5 mg/mm^2. The arc was constricted to allow extensive dissolution when higher 1 mg/mm^2 to 2 mg/mm^2 powder were used and so dissolution and reprecipitation was poor. The populated undissolved TiC above 1 mg/mm^2 deemed for the demarcation hardness trends which were evident by sudden dropped from above 1400 HV to ~ 900 HV and rised back to 1050 HV. Dissolution of substrate and particulates were enhanced with higher heat input associated with lower powder content.

1. Introduction

Steel is common and known as the main element for the component productions serving mostly in the field of aerospace, aeronautical, construction, mining, automotive, railway, oil and gas and shipbuilding industries. The material is favoured because of the low prices, abundant, reliable, adapted to various fabrication and treatment processes and recyclable. Despite this, steel family inherit the poor wear and corrosion properties that makes them suffer material losses especially

* *Corresponding author.*
E-mail address: maleque@iium.edu.my

https://doi.org/10.37934/aram.114.1.3342

when they are brought under extreme services or aggressive environmental. One way to constrain this problem is by composing selective alloying elements such as tantalum, chromium, vanadium, titanium with carbon to form the metal matrix composite layers. The carbides with their respective matrices were very effective to reduce wear because of their hardness [1-8]. The carbide embedment on the surface of steel via TIG or laser beam surface modification processes had been reported to transform the track hardenability several times than the substrate at different melt pool sizes with various microstructural features, population and sizes [7-13]. Using the TIG process, greater TiC amount developed the maximum of 1400 HV from the track that was melted twice than only melting once resulting 900 HV of 1.56 times lower. The two times melting the powder consisting iron, titanium and carbon gave populated TiC on the mild steel substrate hence enhanced surface hardenability [14]. Laser melting the titanium, graphite and iron powders on the mild steel substrate produced dendritic structure near top layer and at the bottom, the TiC particles were embedded in the steel matrix [15]. With TiC particulates, they endeavored dissolution followed by reprecipitation of carbides in the form of dendrites, cubic or globular structures associated with the undissolved ones embedded in the melt pools [16,17]. Melting with the low heat input lead for the fabrication of small molten pool containing high amount of carbides [18]. Precipitation of carbides were much low in sizes and many, when greater carbon content was employed during melting [19]. Of indentations made under the Vickers microhardness test, the first one gave 820 HV that had impression resisted by two undissolved TiC and another one, 7 reprecipitated carbide from about 2 µm to 5 µm in sizes resisted the deformation resulting the hardness of 700 HV [20].

In this work, TiC particulate was used to reinforce the surface of the AISI 4340 low alloy steel substrate. TiC was admired to be used as the reinforcement because of their compatibility with steel, high melting temperature, high hardness, good thermal stability and low of coefficient of thermal expansion. No work was found to extensively present the correlation of melt pool sizes, microstructural features, defects and microhardness against the preplaced TiC powder amount and heat inputs. The TiC dispersion and density behaviour within the molten pool via TIG arcing process is yet to be further explored. This work presents the results of preplaced powder content between 0.4 mg/mm^2 to 2 mg/mm^2 using the energy inputs from 1008 J/mm to 2160 J/mm in terms of melt pool sizes, microstructural features, defects and microhardness. The result from this work would provide vital information to replicate TiC metal matrix composite layers via TiG technique for a defect free coating with the high hardness values.

2. Experimental Work

In this work, the AISI 4340 low alloy steel was cut to the dimension of 40 x 100x 15 mm^3. The surface of this substrate was grounded using the silicon carbide (SiC) abrasive paper to remove the rust or the debris followed by cleaning using the detergent and alcohol. The TiC particulates of the sizes between 45 µm to 100 µm was used for the reinforcement. The weighed TiC powder was added with the polyvinyl alcohol (PVA) binder forming thick paste and immediately spread across the AISI 4340 substrate surface using the plastic film. This was followed by evaporating the paste in the oven at 80^{o}C for 1 hour in order to ensure the particulates adhered on the surface of the substrate. Table 1 shows the used energy inputs with respective preplaced powder content on the substrate associated with the formed melt pool sizes and HAZ. Before melting starts, the samples containing different amount of reinforcing particulates were placed underneath the TIG torch with a 1 mm working distance. Those single layer tracks were fabricated using NC Telwin and Miller 165 TIG welding machine from the heat inputs at 1008, 1296 and 2160 J/mm each travelling at 1 mm/s. The

tracks were streamed with argon shielding gas at 20 lit/min to prevent the molten pool against excessive oxidation. Figure 1 shows the illustration describing the preplaced powder TIG process.

Table 1
The geometrical sizes of the molten pool formed by different energy inputs and powder content

Tracks	Voltage (V)	Current (A)	Energy (J/mm)	Powder (mg/mm^2)	Melt depth (mm)	Melt width (mm)	HAZ (mm)
1	30	70	1008	0.4	0.54	2.9	0.87
2	30	70	1008	0.5	0.51	2.8	0.84
3	30	90	1296	0.5	0.79	3.2	1.01
4	45	100	2160	1	1.22	3.8	1.55
5	45	100	2160	1.5	1.07	4.2	1.39
6	45	100	2160	2	1.03	4.5	1.6

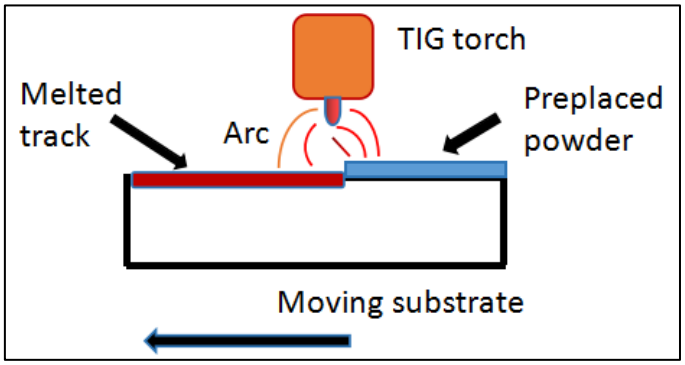

Fig. 1. Illustration describing the melting process using TIG torch against the preplaced powder which is above the substrate

In this work, the equation used to calculate the energy inputs is described elsewhere [21]. After the samples cooled to the room temperature, they were sectioned equally to two pieces followed by preparing them using standard metallography technique for microstructural observation and characterization. Nital solution was used for etching of the few seconds. Nikon 400 mm/L optical microscope was used to determine the melt pool and the heat affected zone (HAZ) sizes. JEOL JSM 5600 scanning electron microscope was used for the microstructural analysis while the EDX attached to this microscope was used to determine the chemical composition of the existing phases. Wilson Wolpert microhardness testing machine was used to determine the hardenability of the sample near the surface away to the undisturbed substrate at an interval of 100 µm. The hardness values were recorded from the indentation made at 500 gf of 10 seconds delay.

3. Result and Discussion

Table 1 shows the geometrical features of the cross sectioned layer consisting melt widths, melt depths and HAZ depth against different powder content and heat inputs. The desolation of the melt layers were seen from the solidified melt front containing carbides resembling melt pool depths and width and the HAZ. The Table shows that the melt pool sizes are classified into two bands. The first band consist the tracks produced below than 1296 J/mm and less than 0.5 mg/mm^2 powder. It can be seen that the 1008 J/mm preplaced with 0.4 mg/mm^2 gave melt depth and width of 0.54 mm and 2.9 mm respectively. With the same energy input the geometrical sizes was lesser preplaced with 0.5 mg/mm^2 resulting 0.51 mm depth and 2.8 mm width seeing these features the lowest among the three tracks. This poor melting condition at 1008 J/mm of 0.5 mg/mm^2 powder content was

overcome by increasing the heat input to 1296 J/mm where the deepest depth of 0.79 mm and width at 3.2 mm prevailed. The first band had the HAZ lengths between 0.84mm to 1.01 mm.

The second band consist three tracks fused at the same 2160 J/mm with increased of powder content from 1 mg/mm^2 to 2 mg/mm$^{2..}$ At 2160 J/mm, the greatest melt size was formed with 1mg/mm^2 having 1.22 mm of depth and when the powder content increases to 1.5mg/mm^2 and 2 mg/mm^2, the distances gradually reduced to 1.07mm and 1.03 mm respectively. The lessening of the melt layer development was also seen from 0.4 mg/mm^2 to as little as 0.5 mg/mm^2 both at 1008 J/mm. The results showed the melt pool expansions were constricted to develop with increased of the TiC content. A way to solve this problem has been seen by increasing the heat input from 1008 J/mm to 1296 J/mm; 0.5 mg/mm^2, which resulted the depth extension at the length of 0.25 mm with 0.4 mm width. Decreasing the working distances and had been reported for the increase of melt dilution [16]. Reports showed more energy was required to melt and enlarged the preplaced WC particulates than the substrate and so melt pool sizes growth were limited using laser [22,23]. Similar phenomenon was also reported elsewhere [24]. In this work, even though the powder contents were as high as 4 times between 1 mg/mm^2 to 2 mg/mm^2 fused at 2160 J/mm realizing constriction to melt than the below 1296 J/mm between 0.4 mg/mm^2 to 0.5 mg/mm^2, yet the geometrical sizes were up to twice with the 2160 J/mm than below 1296 J/mm. This shows that the heat input is the dominant factor that controls the formation of the melt pool sizes.

The microstructure in Figure 2 exhibited the micrographs of the cross sectioned tracks which consist of the melt zone, HAZ and the undisturbed substrate between the heat input of 1008 J/mm to 2160 J/mm of 0.4 mg/mm^2 to 2.0 mg/mm^2 powder content. The melted material followed by the liquid stirring action successfully distributed those reprecipitated and undissolved TiC to be embedded within the melt pool. Those tracks were associated with sound metallurgical bonding against the substrate, upon intensive investigation the samples were formed without any crack defects either on the observed micrographs or along the total length after melting. With the absence of such defects, TiC had exerted its suitable characteristic to be used as a reinforcing material fused under the TIG arc source for a thin AISI 4340 metal matrix composite layer.

Pores were seen especially with the melting produced between 1 mg/mm^2 to 2 mg/mm^2 of 2160 J/mm heat input as indicated by black arrows from Figures. 2iv - vi. Pores were formed by the escaped gas from the burnt binder used to adhere the TiC particulates on the surface of the substrate. Introducing more preplaced powders were associated with increased of used PVA binder which led to the released of the high amount of gasses in the presence of viscous melt. This is why the 2 mg/mm^2 (highest binder content) to retain many trapped pores within the molten pool compared to the 1 mg/mm^2 of the same fused energy. Reducing the preplaced powder up to 5 times lower to about 0.4 mg/mm^2, gave less spread particulate content with reduced of used binder fused below than 1296 J/mm. This may be the reason for the almost no pores seen within the molten pool from Figures. 2i - iii. The little gasses escaped before the metal solidifies favors the track produced below than the 1296 J/mm heat inputs. The formation of pores phenomenon were reported in several surface melting works that used powder preplacement as the reinforcing style [16,25-27].

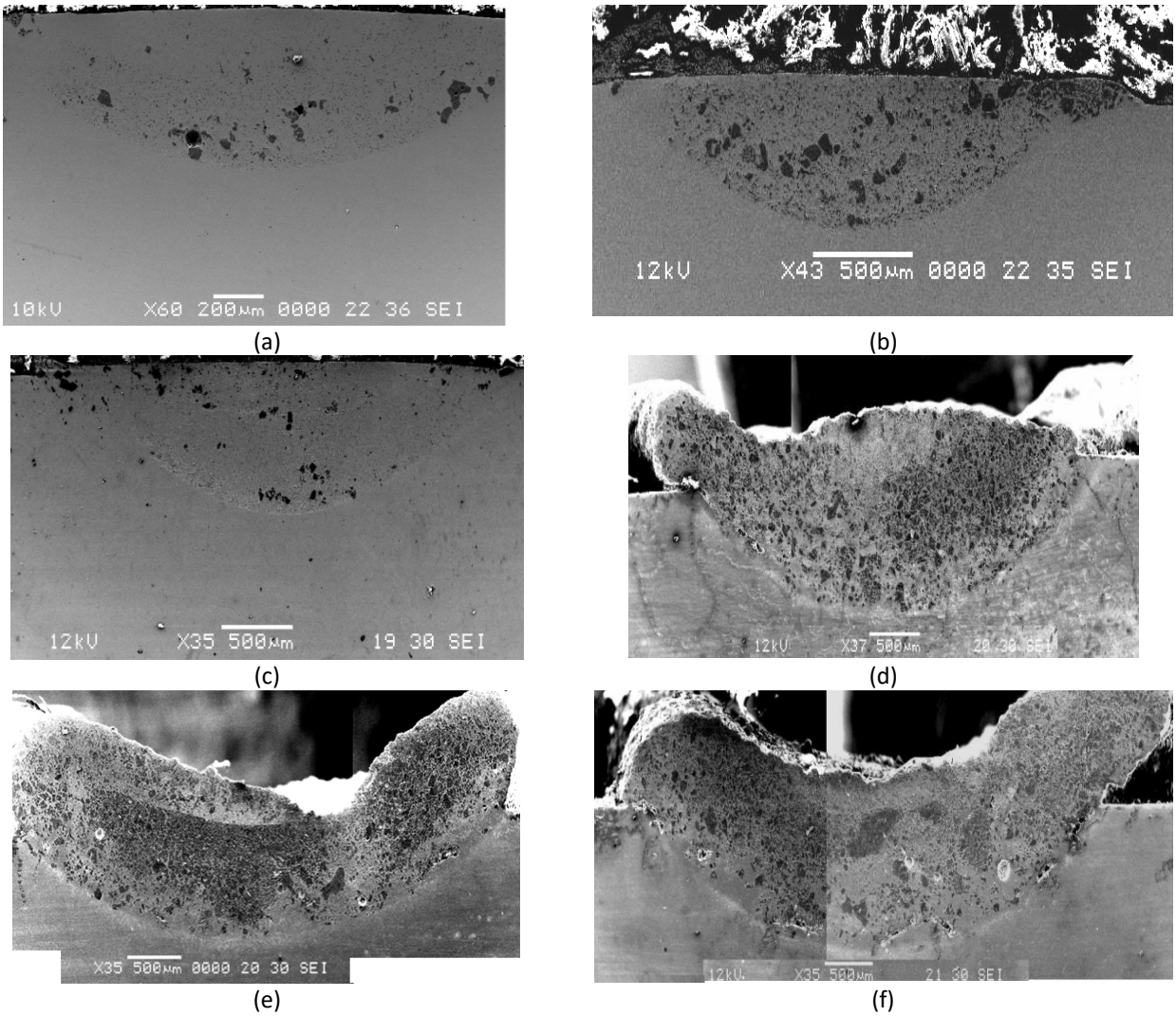

Fig. 2. Micrograph showing the melt pool formed at 1008 J/mm with 0.4 mg/mm^2 (a) 1008 J/mm with 0.5 mg/mm^2 (b) 1296 J/mm with 0.5 mg/mm^2 (c) 2160 J/mm with 1 mg/mm^2 (d) 2160 J/mm with 1.5 mg/mm^2 (e) and 2160 with 2.0 mg/mm^2 (f) White arrows showing pores

All melted pool formed the hemispherical shape testifying the Gaussian energy distribution of arc intensity which was the highest at the center and gradually reduced to the left and right edges. Reports describing the Gaussian energy distribution of Evident from the highest heat intensity was seen from the highest melt depths in the middle followed by thickness reduction to both edges. The produced hemispherical melt shape due to the Gaussian energy distribution was reported using TIG and laser [16,22] In general, the tracks produced at 1008 J/mm and 1296 J/mm with 0.4 mg/mm^2 and 0.5 mg/mm^2 respectively exhibited almost complete dissolution of TiC particles. The dark spots of undissolved carbide were clearly indicated with the 1008 J/mm of 0.5 mg/mm^2. However, processing between 1 to 2 mg/mm^2 at higher energy input of 2160 J/mm were poor to melt those particulates evident from the dissemination most of the undissolved particulates over the sample surface. Even so, highest dilution is noticeable with 1 mg/mm^2 sample than those up to 2 mg/mm^2 which explained that the resistance to melt was due to the addition of excessive powder content that reduces the efficiency to melt. The presence of those undissolved particulates within the matrix with precipitation at places) showed the melts were in the semi-solid state. The dissolution were seen more effective when applying the heat input below 1296 J/mm between 0.4 to 0.5 mg/mm^2. Applying the heat input of 1296 and 2160 J/mm with 0.5 mg/mm^2 and 1 mg/mm^2 respectively were the best combination

that introduced dissolution compared to their rival tracks. Indicated by more of the undissolved particulates, less dissolution were assured by melting at 1008 J/mm with 0.5 mg/mm^2 (Figure2ii) and 2160 with 2 mg/mm^2 (Figure 2vi) among their rival. The result suggest that it would require the right proportion of powder content and heat input to tailor or favour complete TiC dissolution or homogeneously mixed between the precipitated and undissolved TiC or dominance of TiC particulates with traces of precipitated ones. Not only the heat input and powder content, altering the working distances or using difference of shielding gasses may deliver various content,type, sizes of microstructural features within tracks [16,28]. The lesser the particles with increased of energy input, the better the dissolution is.

The micrograph of the sample fused at the 1008 J/mm and 0.4 mg/mm^2 powder with the EDX elemental results observed on a TiC precipitate and the matrix phase are shown in Figure 3. Figure 3(i) shows the melt consisted of Fe matrix embedded with those reprecipitated globular, flower and cubic type of TiC just above the HAZ. The micrograph also evident that the melt within this region was in the phase of liquid since no undissolved particulates were presence. Here, the liquid temperature exceeded over than 3600^{o}C which was the melting temperature of TiC particulates and so dissolution took place followed by precipitation of 0.4 mg/mm^2 track. Difference of morphological features of cubic and globular (Figure 3i) than the undissolved particulates (Figure 4) and far from the as-received 45 - 100 µm powder sizes are additional information that had TiC dissolved followed by precipitation.

The extent of TiC particles dissolution tailors the amount of the reprecipitated TiC density and dispersion. Dissolved TiC at higher amount with the presence of longer solidification time resulted armed dendritic microstructure. Reprecipitated TiC was formed by dissolved particulates with Fe and upon solidification Ti and C combined and emerged as globular, flower or cubic type of structures. The composition of the TiC phase was confirmed by the EDX analysis for the flower precipitates in Figure 3 (i) consisting of an association between Ti and C as shown by the spectra in Figure 3 (ii). The matrix had the major element of Fe with little of Ti for the solid solution strengthening in Figure 3 (iii). Figure 4 shows a cracked undissolved particulate. Just like those the reprecipitated ones in Figure 3, this particulate was seen well bonded against the matrix. Due to the cracking, liquid matrix successfully infiltrated through the formed cavity as shown in Figure 4. by an arrow. The thermal shock caused by abrupt heating and sudden cooling during solidification was responsible to cause such phenomenon. In a literature, SiC cracking behaviour was reported when incorporated with the Ti-6Al-4V substrate under laser due to the difference of thermal of coefficient expansion between that of SiC and titanium [29].

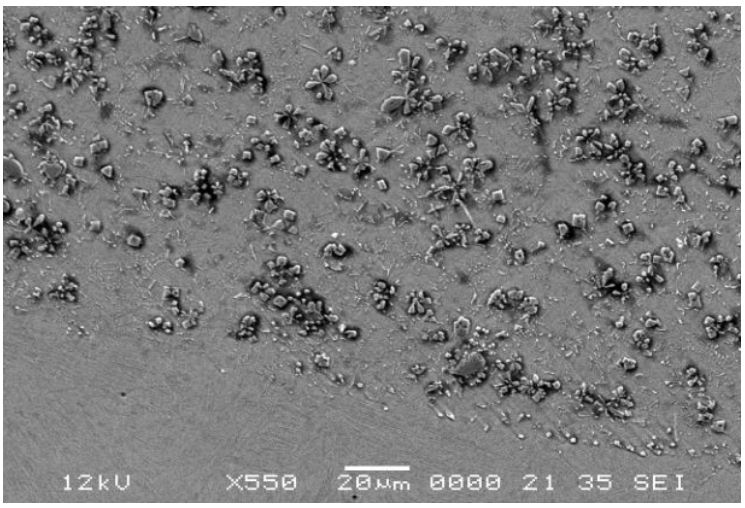

(a)

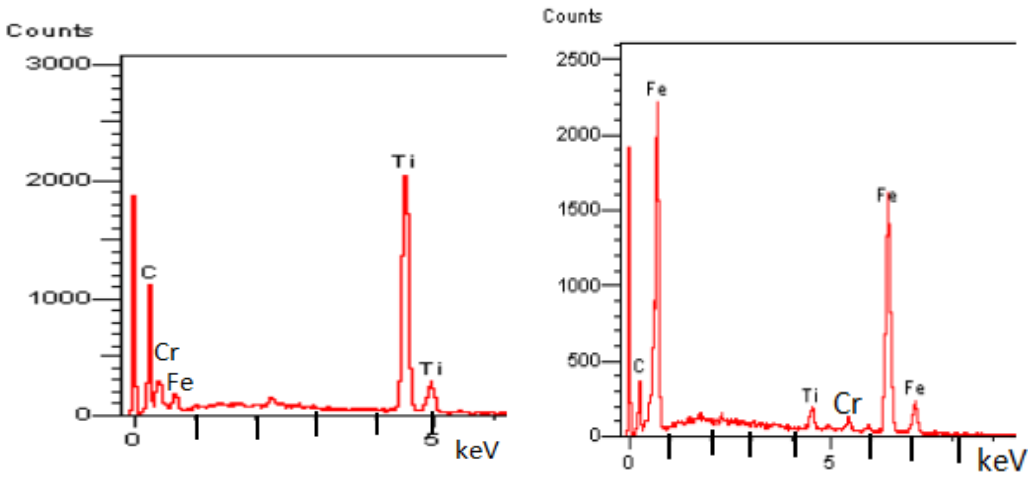

(b) (c)

Fig. 3. Micrograph of the TiC precipitates near the melt matrix interphase containing 0.4 mg/mm^2 of 1008 J/mm with the EDX analysis results (a) locates the flower precipitates and the solid solution matrix by arrows used for the EDX analysis with their results in (b) and (c) respectively

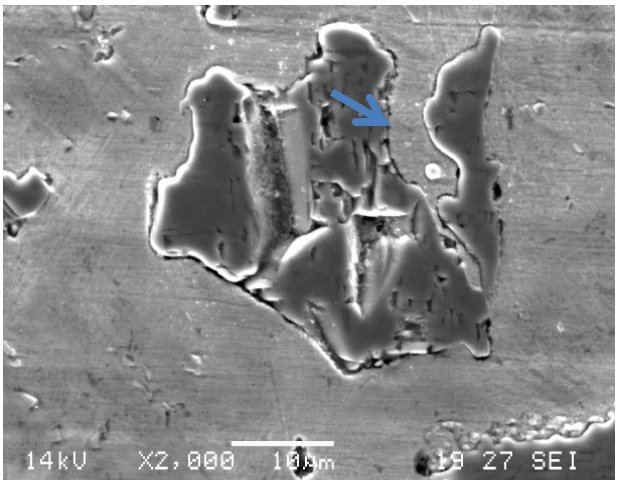

Fig. 4. A cracked particulate with an arrow showing matrix infiltration

The microhardness profile of the produced tracks below than 1296 J/mm and at 2160 J/mm of various powder content is shown in Figure 5. The graph depicted the formation of TiC metal matrix composite layer produced microhardness between 600 HV to almost 1600 HV. The martensitic HAZ remained between 500 HV to 600 HV while the undisturbed substrates were consistent in values of about 300 HV. Even though with small melt sizes (Table 1), the less containment of TiC within the pool gave lower hardness between 600 HV to 900 HV fused below 1296 J/mm. The melt size expansion that was thought to reduce the microhardness is compensated by the filling of more carbide preplaced between 1 mg/mm^2 to 2 mg/mm^2 resulting hardness to increase tremendously. The microhardness profile below than 1296 J/mm tracks showed reduction of values with increased of their melt depths. The gradual hardness decrement was because of the gradual reduction of reprecipitated TiC content towards the melt matrix interphase. During fabrication the low density of TiC than the steel made the material to float towards the surface during melting and with the presence of the longest cooling time near the arc source, dissolution was high and masses of TiC reprecipitation took place. This is why hardness was a little higher near the surface. The low temperature region which was at the bottom of the melt had thick solution and prior to this, the melt

suddenly solidifies whilst preventing the dissolution of TiC particulates and generation of reprecipitated TiC structures.

The demarcation trend with those 2160 J/mm layers witnessed abrupt rised over than 1300 HV to certain melt depths followed by sudden drops near 900 HV in Figure 5. These were the evidences of the existence of agglomeration at places with those at 2160 J/mm. The TiC content (0.5 mg/mm^2) fused near the surface at 1008 J/mm gave comparable hardenability than at the lowest 1 and 2 mg/mm^2 depths. When reprecipitation dominates, populated carbide region near the surface at 0.5 mg/mm^2 was hardened similar than those agglomerated regions at the lowest depth (near melt matrix interphase) of 1 and 2 mg /mm^2. Only the 1.5 mg/mm^2 at 2160 J/mm samples showed the near constant hardness trend across the depth.

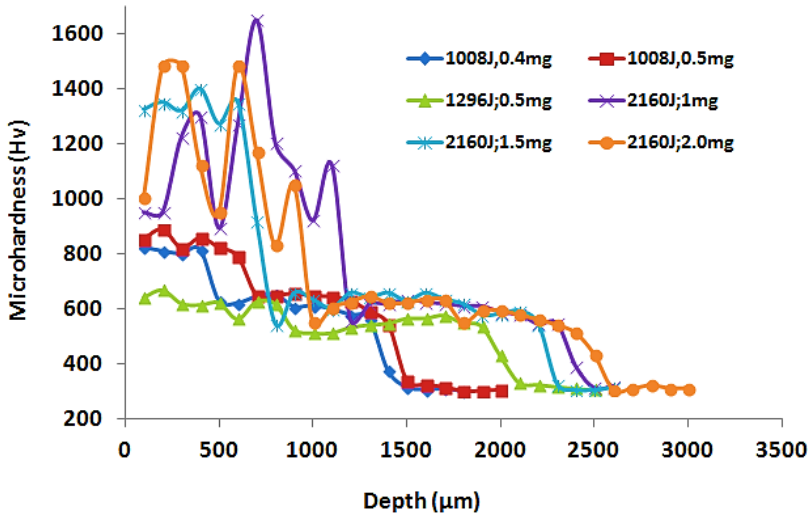

Fig. 5. The microhardness profile of the produced tracks

The persistency of the dense carbide layer were seen from the surface reaching the melt matrix interphase from Figure 2iv-vi. This shows that melting underwent fast solidification which refrained for dissolution leading hardness on all 2160 J/mm tracks for the very high ones. It would require the TiC to efficiently dissolved and reprecipitate either as cubic globular or dendritic structures in order to have gradual hardness reduction just like those below than 1296 J/mm. The tracks with the high TiC particulates had not been dissolved can be overcome by remelting them over again. It is the way for decreasing undissolved or partially dissolved particles whilst having more reprecipitated ones at greater matrix dilution. The above explanation shows that hardness can be tailored to suit special needs of application. It is to be noted that the density of TiC upon solidification is at 4.93 g/cm^3 which is far lighter than the steel at 7.86 g/cm^3. While maintaining high hardenability at the surface layer, forming TiC phase is a way to reduce the material weight.

4. Conclusions

Numerous tracks consisting different content of TiC were succesfully fabricated on the surface of the AISI 4340 low alloy steel substrate using the TIG melting technique. All tracks contain no defect of cracks and their metallurgical bonding to the substrate surface were excellent. The track melt depths were found to decrease with increasing of TiC preplaced content. High preplaced powder amount resulted constriction for the arc to penetrate and melt for large melt pool sizes. Dissolved TiC particulates formed globular and flower types of reprecipitated dispersed carbide with Fe matrix domination diluted from the substrate fused both at the 0.4 mg/mm^2 and 0.5 mg/mm^2 powder

content. The poor fusion between 1 mg/mm^2 to 2 mg/mm^2 at 2160 J/mm rather resulted overwhelmingly undissolved particulates to be dominant. The TiC metal matrix tracks developed hardness approximately 600 HV to 1600 HV which were 2 to 5.3 times higher than the substrate at about 300 HV. The gradual hardness reduction below than 1296 J/mm at 0.4 and 0.5 mg/mm^2 was due to the gradual decreased of reprecipitated TiC content reaching the melt matrix interphase up to the depth of 800 µm. Redundant by many agglomerated undissolved particulates spanning across the molten pool prevailed the demarcation trend of microhardness from as low as 700 HV to 1600 HV fused at 2160 J/mm

Acknowledgement
The financial support for this research was provided by the Ministry of Higher Education Malaysia under the Fundamental Research Grant Scheme (FRGS) with project code FRGS/1/2021/TK0/UIAM/01/1. Authors also thanks to the International Islamic University of Malaysia (IIUM) for technical supports that made this study possible.

References

[1] Candela, C.Sánchez de Rojas, Riquelme, Ainhoa., Rodrigo, Pilar., Torres, Belén., , Rams, Joaquin. "Wear behaviour of additively manufactured 316L/SiCp composites with up to 60 wt% SiCp." *Ceramic International* 48, no. 22 (2022): 33736-33750. https://doi.org/10.1016/j.ceramint.2022.07.319
[2] Bedolla-Becerril, Egberto, Josefina Garcia-Guerra, Víctor H. Lopez-Morelos, Marco A. Garcia-Renteria, Lazaro A. Falcon-Franco, Víctor H. Martinez-Landeros, Sergio García-Villarreal, and Sergio E. Flores-Villaseñor. "Tribological Behaviour of Al-2024/TiC Metal Matrix Composites." *Coatings* 13, no. 1 (2022): 77. https://doi.org/10.3390/coatings13010077
[3] Li, Chonggui, Shuai Li, Chuanming Liu, Youfeng Zhang, Peiran Deng, Yajun Guo, Jinqian Wang, and You Wang. "Effect of WC addition on microstructure and tribological properties of bimodal aluminum composite coatings fabricated by laser surface alloying." *Materials Chemistry and Physics* 234 (2019): 9-15. https://doi.org/10.1016/j.matchemphys.2019.05.089
[4] Zorzi, Janete Eunice, Cláudio Antônio Perottoni, and J. A. H. Da Jornada. "Hardness and wear resistance of B4C ceramics prepared with several additives." *Materials Letters* 59, no. 23 (2005): 2932-2935. https://doi.org/10.1016/j.matlet.2005.04.047
[5] Ren, Yiqun, Liqun Li, Yuandong Zhou, and Shuliang Wang. "In situ synthesized VC reinforced Fe-based coating by using extreme high-speed laser cladding." *Materials Letters* 315 (2022): 131962. https://doi.org/10.1016/j.matlet.2022.131962
[6] Debta, Malaya Kumar, and Manoj Masanta. "Effect of stand-off-distance on the performance of TIG cladded TiC-Co coating deposited on Ti-6Al-4V alloy." *Surface and Coatings Technology* 434 (2022): 128210. https://doi.org/10.1016/j.surfcoat.2022.128210
[7] Serope Kalpakjian and Steven R. Schmid. Manufacturing Engineering and Technology, 5th edition, Prentice Hall, 123.
[8] Shahbudin, Siti Nurshahmira Ahmad, Sri Yulis M. Amin, Mohd Hilmi Othman, and Mohd Halim Irwan Ibrahim. "Study on Properties of Heat-treated WC-6Co with Different Wt.% of TiC Powder." *Journal of Advanced Research in Fluid Mechanics and Thermal Sciences* 66, no. 2 (2020): 168-178..
[9] Idriss, Ahmed Nazrin Md, Salmiah Kasolang, M. A. Maleque, Ramdziah Md Nasir, and Nibong Tebal. "An overview on the importance of surface modification by TIG and lasers incorporating carbides and their relations to wear behaviours." *Jurnal Tribologi* 29 (2021): 96-116.
[10] Ayers, J. D. "Wear behavior of carbide-injected titanium and aluminum alloys." *Wear* 97, no. 3 (1984): 249-266. https://doi.org/10.1016/0043-1648(84)90152-2
[11] Lusquiños, F., R. Comesaña, A. Riveiro, F. Quintero, and J. Pou. "Fibre laser micro-cladding of Co-based alloys on stainless steel." *Surface and Coatings Technology* 203, no. 14 (2009): 1933-1940. https://doi.org/10.1016/j.surfcoat.2009.01.020
[12] Dyuti, Sarker, S. Mridha, and S. K. Shaha. "Wear behavior of modified surface layer produced by TIG melting of preplaced Ti powder in nitrogen environment." *Advanced Materials Research* 264 (2011): 1427-1432. https://doi.org/10.4028/www.scientific.net/AMR.264-265.1427
[13] Kirchgaßner, M., E. Badisch, and F. Franek. "Behaviour of iron-based hardfacing alloys under abrasion and impact." *Wear* 265, no. 5-6 (2008): 772-779. https://doi.org/10.1016/j.wear.2008.01.004

[14] Wang, X. H., S. L. Song, Z. D. Zou, and S. Y. Qu. "Fabricating TiC particles reinforced Fe-based composite coatings produced by GTAW multi-layers melting process." *Materials Science and Engineering: A* 441, no. 1-2 (2006): 60-67. https://doi.org/10.1016/j.msea.2006.06.015

[15] Emamian, Ali, Stephen F. Corbin, and Amir Khajepour. "The influence of combined laser parameters on in-situ formed TiC morphology during laser cladding." *Surface and Coatings Technology* 206, no. 1 (2011): 124-131. https://doi.org/10.1016/j.surfcoat.2011.06.062

[16] Idriss, AN Md, M. A. Maleque, and A. Afiq. "Synthetization of TiC surface hardening using TIG melting technique-The effect of working distance." In *IOP Conference Series: Materials Science and Engineering* 1244, no. 1 (2022): 012012. https://doi.org/10.1088/1757-899X/1244/1/012012

[17] Mridha, Shahjahan, and T. N. Baker. "Overlapping tracks processed by TIG melting TiC preplaced powder on low alloy steel surfaces." *Materials Science and Technology* 31, no. 3 (2015): 337-343. https://doi.org/10.1179/1743284714Y.0000000530

[18] Toozandehjani, M., F. Ostovan, E. Shafiei, K. R. Jamaludin, A. Amrin, and E. Hasanzadeh. "Surface treatment of Al7075 Matrix by TiC particles via hybrid ball milling and tungsten inert gas cladding." *Metall Ital.* 2020 (2020): 21-30.

[19] Chang, Chia-Ming, Yen-Chun Chen, and Weite Wu. "Microstructural and abrasive characteristics of high carbon Fe–Cr–C hardfacing alloy." *Tribology international* 43, no. 5-6 (2010): 929-934. https://doi.org/10.1016/j.triboint.2009.12.045

[20] Idriss, AN Md, S. Kasolang, and M. A. Maleque. "Demographic Changes by the Vickers Microhardness Surface Indentations on the TiC Metal Matrix Composite TIG Melted Track." In *Proceedings of the Malaysian International Tribology Conference*, (2020): 230-235. https://doi.org/10.1007/978-981-16-9949-8_42

[21] Easterling, K.E. Chapter 1 - Introduction to the Physical Metallurgy of Welding. Butterworth - Heinemann, London. (1995).

[22] Salleh, Muhammad Naqiuddin Mat, Mahadzir Ishak, Kazuhiko Yamasaki, Moinuddin Mohammed Quazi, and Aiman Mohd Halil. "Pulsed Nd: YAG laser parameters effect on welding uncoated advance high strength steel (AHSS) for automotive." *Journal of Advanced Research in Fluid Mechanics and Thermal Sciences* 84, no. 1 (2021): 91-100.https://doi.org/10.37934/arfmts.84.1.91100.

[23] Li, Chonggui, Shuai Li, Chuanming Liu, Youfeng Zhang, Peiran Deng, Yajun Guo, Jinqian Wang, and You Wang. "Effect of WC addition on microstructure and tribological properties of bimodal aluminum composite coatings fabricated by laser surface alloying." *Materials Chemistry and Physics* 234 (2019): 9-15. https://doi.org/10.1016/j.matchemphys.2019.05.089

[24] Amuda, M. O. H., T. F. Lawal, O. Daramola, and A. B. W. O. Awarun. "Wear and corrosion characteristics of silicon carbide surface modified mild steel." *UNILAG Journal of Medicine, Science and Technology* 6, no. 1 (2018): 129-146.

[25] Abboud, J. H., and D. R. F. West. "Microstructure of titanium injected with SiC particles by laser processing." *Journal of Materials Science Letters* 10, no. 19 (1991): 1149-1152. https://doi.org/10.1007/BF00744110

[26] Mridha, S., and T. N. Baker. "Incorporation of 3 µm SiCp into Titanium surfaces using a 2.8 kW laser beam of 186 and 373 MJ m− 2 energy densities in a nitrogen environment." *Journal of materials processing technology* 185, no. 1-3 (2007): 38-45. https://doi.org/10.1016/j.jmatprotec.2006.03.110

[27] Mridha, Shahjahan, AN Md Idriss, and T. N. Baker. "Incorporation of TiC particulates on AISI 4340 low alloy steel surfaces via tungsten inert gas arc melting." *Advanced Materials Research* 445 (2012): 655-660. https://doi.org/10.4028/www.scientific.net/AMR.445.655

[28] Muñoz-Escalona, P., Shahjahan Mridha, and T. N. Baker. "Effect of shielding gas on the properties and microstructure of melted steel surface using a TIG torch." *Advances in Materials and Processing Technologies* 1, no. 3-4 (2015): 435-443. https://doi.org/10.1080/2374068X.2015.1133789

[29] Das, Mitun, Sandip Bysakh, Debabrata Basu, TS Sampath Kumar, Vamsi Krishna Balla, Susmita Bose, and Amit Bandyopadhyay. "Microstructure, mechanical and wear properties of laser processed SiC particle reinforced coatings on titanium." *Surface and Coatings Technology* 205, no. 19 (2011): 4366-4373. https://doi.org/10.1016/j.surfcoat.2011.03.027